Applied Catalysis B: Environmental 83 (2008) 208–213

Contents lists available at ScienceDirect

Applied Catalysis B: Environmental

journal homepage: www.elsevier.com/locate/apcatb

Synthesis of nanosized biogenic magnetite and comparison of its catalytic activity in ozonation

Haeryong Jung [1], Jung-Woo Kim, Heechul Choi *, Ji-Hoon Lee, Hor-Gil Hur

Department of Environmental Science and Engineering, Gwangju Institute of Science and Technology (GIST), 1 Oryong-dong, Buk-gu, Gwangju 500-712, South Korea

ARTICLE INFO

Article history:
Received 17 July 2006
Received in revised form 14 February 2008
Accepted 19 February 2008
Available online 26 February 2008

Keywords:
Biogenic iron oxide
Magnetite
Ozonation
Catalytic reaction
*p*CBA

ABSTRACT

Nanosized biogenic iron oxide was synthesized by dissimilatory iron-reducing bacterium, *Shewanella* sp. This biogenic iron oxide was evaluated as a catalyst in the heterogeneous catalytic ozonation of *para*-chlorobenzoic acid (*p*CBA). XRD and TEM analyses showed that the biogenic iron oxide was magnetite phase (Fe_3O_4) and was composed of nanosized irregular particles in the range of 10.0 ± 4.0 nm in diameter. Catalytic ozonation was carried out at acidic pH levels (~2.5) in the presence of the biogenic magnetite. It was clearly shown that the biogenic magnetite enhanced the degradation of *p*CBA by the production of $^{\bullet}OH$ resulting from the catalytic decomposition of ozone on the surface of the particles. Functional groups on the surface of the biogenic magnetite played a role of catalytic active sites, and this was confirmed by FT-IR and titration analyses. However, the biogenic magnetite showed a lower catalytic efficiency than the commercial nanosized magnetite, resulted from the formation of 4 times bigger aggregates of the biogenic magnetite than the commercial one in aqueous solutions. The R_{ct} values representing the ratio of hydroxyl radicals and ozone were found to be divided into two regions during reaction. The R_{ct} values during first period (1 min) were much greater than those during second period, and this was caused by initial rapid decrease of *p*CBA.

1. Introduction

It has been clearly demonstrated that metal catalysts can effectively be utilized to improve the ozonation efficiency for the removal of a number of organic compounds [1,2]. In particular, solid metal oxides are more useful in catalytic ozonation than ionized metals, as ionized metals are considered toxic substances in water. Beltran et al. [3] further reported that ozone efficiency in heterogeneous catalytic ozonation was higher than that found in homogeneous catalytic ozonation. Our previous work also indicates that heterogeneous catalytic ozonation using microsized FeOOH enhances the degradation of ozone and *para*-chlorobenzoic acid (*p*CBA) [1].

Iron oxides and hydroxides have been used in the catalytic ozonation due to advantages, such as their abundance on earth and their stable form [4]. These materials represent 6% of the chemical composition of the Earth's crust [5]. Specifically, nanosized iron oxides are drawing a great deal of attention in chemical and biological processes because of following reasons: (1) nanosized particles have larger surface area/volume ratios than bulk materials for a given amount; and (2) the structure of the nanosized iron oxide surface may differ from those of bulk materials. Hence, reducing the diameter of iron oxides to nanometer size could enhance the reactivity.

Nanosized iron oxides have been synthesized by using various synthesis methods, such as electrochemical, sol–gel, and thermal decomposition methods; however, these methods generally use toxic and expensive chemicals as reactants or complex devices or high-energy cost. For example, the thermal decomposition method requires toxic organic solvents and surfactant to be heated up to 320 °C, producing toxic wastes during the process. To this extent, the biomineralization could be considered as an effective alternative for the synthesis of nanosized iron oxide, as it is both environmentally friendly and cost-effective. Specifically, magnetite (Fe_3O_4) can be formed by a diversity of organisms; here two different types of biogenic magnetite are reported: biologically induced magnetite and biologically controlled magnetite. Biologically controlled magnetite is a biomineral comprised of highly ordered crystals, whereas biologically induced magnetite is extracellularly produced biomineral that does not crystallize under strict genetic control [6]. The amount of biologically controlled magnetite produced is very small, because it is synthesized within microorganisms. For this study, we synthesized

* Corresponding author. Tel.: +82 62 970 2441; fax: +82 62 970 2434.
E-mail address: hcchoi@gist.ac.kr (H. Choi).
[1] Present address: Radwaste Disposal Research Team, Nuclear Engineering & Technology Institute (NETEC), Korea Hydro & Nuclear Power Co. LTD., 25-1 Jang-dong, Yuseong-gu, Daejeon 305-343, South Korea.

0926-3373/$ – see front matter © 2008 Elsevier B.V. All rights reserved.
doi:10.1016/j.apcatb.2008.02.016

biologically induced magnetite from iron-reducing bacterium for the application of a heterogeneous catalyst.

In this paper, we focus on: (1) the synthesis and characterization of nanosized biogenic iron oxide for the application as a heterogeneous catalyst in ozonation; and (2) the efficiency evaluation of nanosized biogenic iron oxide in heterogeneous catalytic ozonation. The experimental results with the biogenic iron oxide were compared with those of chemically similar commercially available iron oxide.

2. Methods

2.1. Chemicals

All chemicals were obtained in high purity and were used as received. Ethanol and hexane were purchased from Duksan Chem. (South Korea). *para*-chlorobenzoic acid (*p*CBA) was purchased from Aldrich (Milwaukee, Wisconsin, USA). All solutions were prepared by using deionized water (Ultrapure system, Barnsterd).

2.2. Biomineralization of iron oxides

Biogenic iron oxide was produced by dissimilatory iron-reducing bacterium, *Shewanella* sp. The bacterium was incubated in anaerobic conditions for 1 month at 30 °C, in the presence of β-FeOOH as a precursor. As previously mentioned, we synthesized the biologically induced magnetite; details are described elsewhere [7]. Biogenic iron oxide was washed before use more than 4 times using deionized water. Commercially available nanosized iron oxide was also purchased from Aldrich (Milwaukee, Wisconsin, USA) for use in a catalytic activity comparison with biogenic magnetite.

2.3. Catalytic ozonation experiments

Batch experiments were carried out with a 1000 mL reactor. The desired volume of *p*CBA and nanosized iron oxide was added to the reactor. The solution was continuously stirred with a magnetic stirrer at 150 rpm, and the desired concentration of gaseous ozone was bubbled in the reactor. The use of a phosphate buffer was avoided in order to control the pH level, as the phosphate buffer could hinder the catalytic reaction on the surface of the catalyst. Hence, either an HCl or NaOH solution was used to control the pH level during the reaction.

Gaseous ozone was generated from pure oxygen by an ozone generator (PCE-WEDECO, GL-1, USA). After a designated time interval, 3 mL of the solution in the reactor was sampled to determine the concentration of *p*CBA. After sampling, an aliquot of 0.1 N $Na_2S_2O_3$ was added to the sample for *p*CBA analysis to quench the aqueous ozone remaining in the reaction solution. Triplicate experiments were conducted at 25 ± 1 °C for verification of all results.

2.4. Characterization of iron oxides and analysis

The synthesized nanoparticles were characterized by transmission electron microscopy (TEM), X–ray diffraction (XRD), field emission scanning electron microscopy-energy dispersive X-ray (FE-SEM-EDX), Fourier transform infrared spectroscopy (FT-IR), and surface area by gas adsorption (BET).

TEM analysis was performed using a JEOL JEM 2000FXII operated at 200 kV. Samples distributed in ethanol were mounted on cupper grids. These cupper grids were kept in oven at 100 °C prior to insertion into the microscope. XRD analysis was performed in ambient air with Cu Kα using a Rigaku RINT2000 wide angle goniometer operated at 40 kV and 40 mA. Continuous scans from 10 to 80°2θ were collected. BET (Brunauer–Emmett–Teller) surface areas were determined from N_2 physisorption with ASAP 2020, using the multi-point BET method. Before each measurement, samples were pretreated at 300 °C for 8 h. EDX analysis was carried out to estimate the normalized element composition of iron oxide nanoparticles using FE-SEM (S-4700, Hitachi, Japan) with EDX (Horiba, Japan). The EDX spectrometer was equipped with a lithium-drifted silicon detector of ultra thin window which allows X-ray detection from the elements with atomic number higher than that of beryllium ($Z > 4$). Electrokinetic mobility was measured using an electrophoretic light scattering spectrophotometer (ELS-8000, Otsuka, Japan). Nanoparticles were diluted in 5 Mm NaCl solution at room temperature. Volumetric titration was also performed using a 702 SM Titrino (Metrohm, Swiss) using potentiometric titration. The titrations were done to estimate the acidic and basic group contents of the nanoparticles in an N_2 atmosphere at a constant temperature of 25 °C with 50 mL of diluted 5 mM iron oxide suspensions in deionized water. The sample was prepared by suspending 57.9 mg of each iron oxide to 50 mL of deionized water. Basic and acid groups were determined using 0.05 N HCl and NaOH solution, respectively. The FT-IR spectra were taken at 1 cm^{-1} resolution in the range of 4000–400 cm^{-1} by an infrared spectrometer (JASCO, FT-IR-460).

*p*CBA was measured by using high performance liquid chromatography (HPLC, WATERS, USA) with an autosampler, a UV absorbance detector (Younglin, UV 730D, South Korea). Details are mentioned elsewhere [2].

3. Results and discussion

3.1. Structure and composition of bacterial iron oxides

XRD patterns of the iron oxides are shown in Fig. 1. As can be seen, it is clear that the synthesized and commercial iron oxides are magnetite phase. Though biologically induced magnetite is typically poorly crystalline and impure [7], the biogenic magnetite synthesized in this study was well crystallized, although some amorphorous phase peaks were observed. In the comparison of the XRD patterns of the biogenic and commercial iron oxides, the commercial iron oxide peaks appear a little broader, indicating a smaller particle size. This was confirmed by both the TEM and BET results.

TEM images were used to determine the shape and size of the iron oxides. As seen in Fig. 2, the biogenic magnetite is composed of nanosized irregular particles. As listed in Table 1, its average size was 10.0 ± 4.0 nm in diameter, and the particles are aggregated into

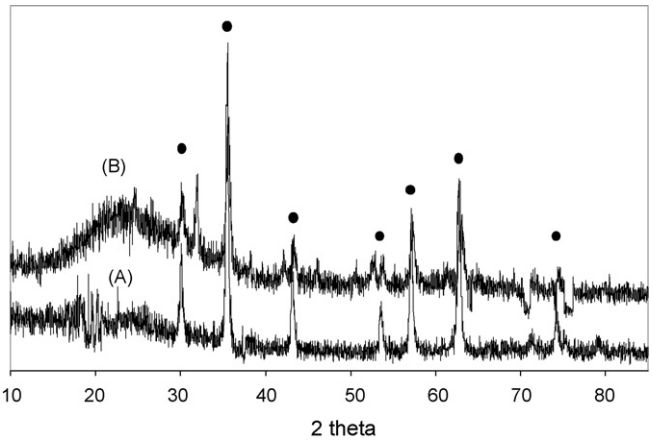

Fig. 1. XRD patterns of iron oxides: (A) commercial iron oxide (B) biogenic iron oxide ((●) Fe_3O_4 magnetite).

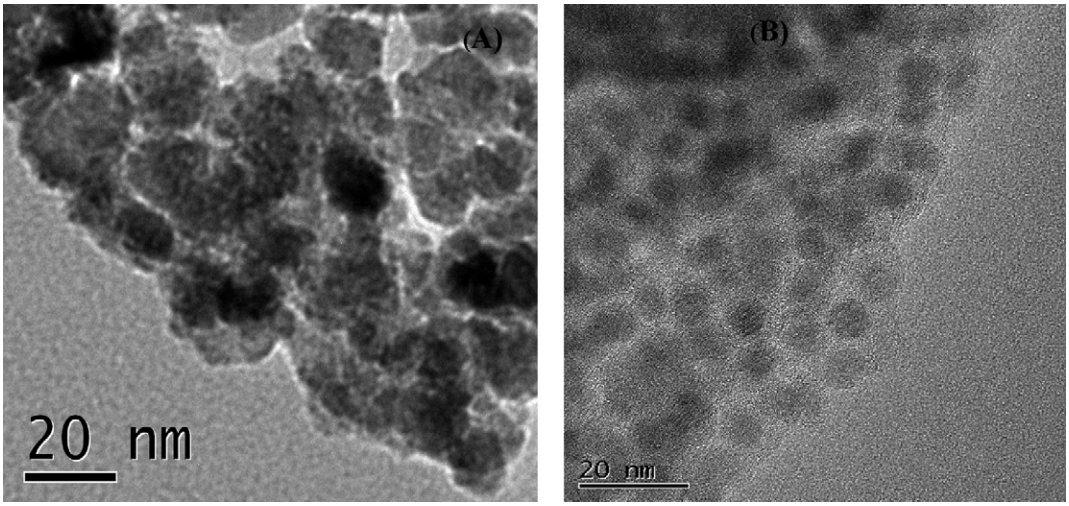

Fig. 2. TEM images of iron oxides: (A) biogenic iron oxide, and (B) commercial iron oxide.

Table 1
Characteristics of nanosized iron oxides.

Name	pH_{iep}[a]	Basic group content[b] (μeq/g)	Particle size (nm)[c]	Surface area (m^2/g)[d]
Biogenic-Fe_3O_4	5.6	530	10.0 ± 4.0	28
Commercial-Fe_3O_4	6.0	340	6.6 ± 0.6	60 (45.28)[e]

[a] Isoelectric point (IEP) was determined by electrophoretic mobility measurement.
[b] Basic group content was determined by titration method.
[c] Particle size was estimated by particle size distribution.
[d] Surface area was determined by BET adsorption method.
[e] Data informed by manufacturer.

bigger sizes. Amophorous particles were also observed in the biogenic magnetite, and this result is consistent with XRD analysis. The commercial magnetite was regularly shaped, and the average size was 6.6 ± 0.6 nm in diameter. The coefficients of variance, i.e., the standard deviation relative to the mean, of the biogenic and commercial magnetite were 0.40 and 0.09, respectively, indicating that the size of the biogenic magnetite is much more variable than that of the commercial magnetite. This large variance in size is a general characteristic of extracellularly produced biominerals [7].

The catalytic efficiency of solid catalysts depends greatly on the catalyst and its surface properties. The important properties are surface area, mechanical strength, and the presence of active sites, such as acid and base sites [8]. Kasprzk-Hordern et al. [8] also concluded that the main parameter on the catalytic properties of metal oxides is acidity and basicity. Sanchez-Polo et al. [9] reported that the surface contents of the basic groups of solid catalysts are essential in enhancing the transformation of ozone to hydroxyl radicals in the heterogeneous catalytic ozonation due to the electrophilic characteristics of aqueous ozone. For this reason, volumetric titration was performed in order to evaluate the basic group contents of the iron oxides. The results are summarized in Table 1.

The basic group content of the biogenic magnetite was determined to be 530.0 μeq/g. This value is higher than the basic group contents of the activated carbons that were used as solid catalysts in heterogeneous catalytic ozonation and showed 253 and 570 μeq/g of basic group content. This result implies that biogenic magnetite could be a good candidate for a solid catalyst in a heterogeneous catalytic ozonation; however, the commercial magnetite showed a much lower value than that of the biogenic magnetite. The higher basic group content of biogenic magnetite seems to be caused by residual biomaterials on the surface of the particle, even though biogenic magnetite was carefully washed several times with deionized water before use in the experiments to remove residual biomaterials, some fractions of the biomaterials was not removed. This existence is confirmed with FT-IR analysis. As shown in Fig. 3, biogenic magnetite displayed much larger functional groups than the commercial magnetite.

Due to the fact that heterogeneous catalytic reaction takes place on the surface of catalysts, the magnitude of the surface reaction can be determined to be generally proportional to the surface area of the solid catalyst, rather than its mass. As such, surface area is seen as a strong indicator affecting the surface-catalyzed reaction. The commercial magnetite showed a higher surface area than the biogenic magnetite, because it had a smaller average diameter than that of biogenic one.

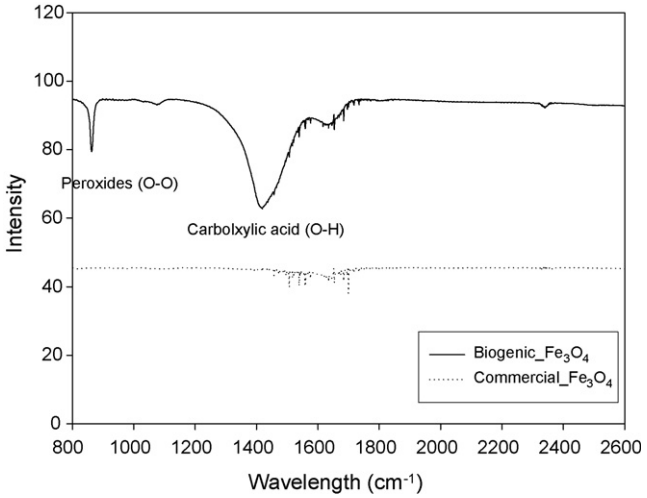

Fig. 3. FT-IR analysis of iron oxides.

Table 2
Normalized element composition in wt.%

Name	Fe/O	Fe	O	C
Biogenic-Fe_3O_4	0.7	38.4	50.9	10.7
Commercial-Fe_3O_4	1.1	48.6	45.1	6.3

FE-SEM-EDX analyses identified the normalized elemental composition of the biogenic and commercial magnetite. EDX data reveals that the biogenic and commercial magnetite is mainly composed of Fe, O, and C, as listed in Table 2. For the biogenic and commercial magnetite, the Fe/O ratios were 0.7 and 1.1, respectively, based on wt.% the Fe/O ratios were 1.5, 1.4, and 1.7, respectively, based on wt.%. These values are significantly less than the ratio of Fe_3O_4 (approx. 3.65). This relatively low Fe fraction and high O fraction may be due to the oxygenated functional groups and/or some carbon fractions formed during the manufacturing process. Furthermore, the biogenic magnetite also exhibited significantly higher O and C fractions, and much lower Fe fraction than Fe_3O_4. The higher O fraction of the biogenic magnetite may be explained by the oxygenated functional groups on the particle surface, such as O–O from peroxidase and O–H from the carboxylic acid functional group. This result is also confirmed by FT-IR spectra; the highest C fraction of the biogenic magnetite seems to originate from the organic residuals of microorganisms.

3.2. Degradation of *p*CBA

Catalytic ozonation was carried out at acidic pH levels (~2.5) in the presence of iron oxides. The initial *p*CBA concentration was controlled in the range of 1–3 mg/L. Fig. 4 presents temporal variations of *p*CBA concentrations at the various concentrations of biogenic magnetite. It was found that the removal rate of *p*CBA increased with an increase in the concentration of the biogenic magnetite. This suggests that the production of hydroxyl radicals was accelerated by the catalytic reaction of ozone on the surface of the biogenic magnetite. As such, the removal of *p*CBA can be divided into two-phases; an initial rapid removal phase of *p*CBA (Phase I), followed by a rather slow decomposition phase (Phase II). Many researchers have reported this pattern of two-stage kinetics in the decomposition of phenanthrene [10], TCE [11], and *p*CBA [2,12] in heterogeneous catalytic ozonation. Hence, in natural water treatment, high levels of hydroxyl radical exposure during Phase I may have partly attributed to apparent fast or near instantaneous formation of bromate, because hydroxyl radicals can significantly contribute to bromate formation [13].

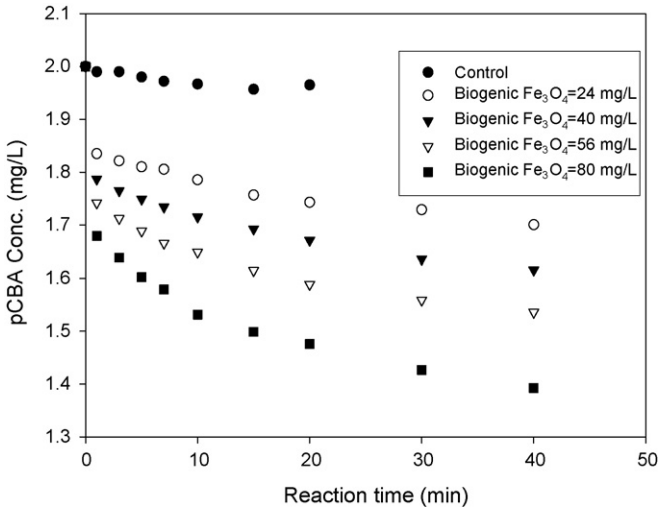

Fig. 4. Effect of iron oxide concentrations on *p*CBA degradation.

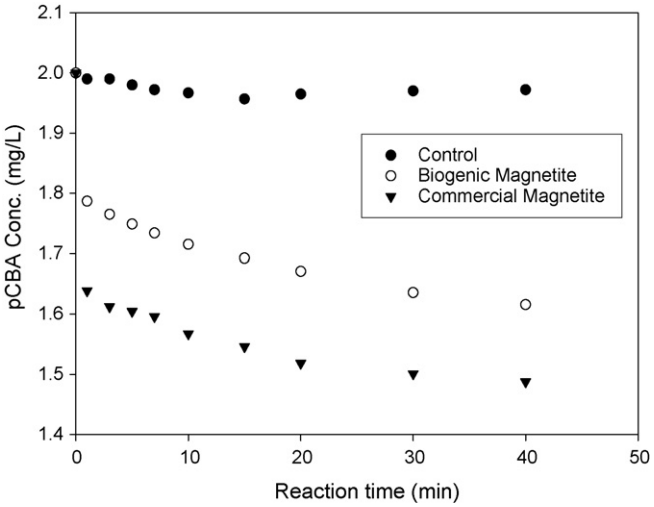

Fig. 5. Effect of particle types on *p*CBA degradation (conc. of iron oxides = 40 mg/L).

In a comparison of particle types, commercial magnetite showed a higher catalytic effect than the biogenic one in the degradation of *p*CBA, as shown in Fig. 5. It is well known that the catalytic effect in heterogeneous catalytic ozonation is proportional to the surface area and basic group contents of the catalyst. The commercial magnetite exhibited higher surface area than the biogenic one; however, its basic group content was lower than that of the biogenic one. Hence, it could be concluded that surface area is mainly responsible for the relatively high catalytic effect in the experimental conditions. However, there is a strong need to re-evaluate the diameter of the nanosized particle in the reactor, because these particles form aggregates and deposition in aqueous solutions [14]. This significantly changes the surface area. For this reason, the particle size in the reactor was measured by using dynamic light scattering (DLS, ELS-8000, Otsuka, Japan). In general, the aggregation characteristics of nanosized particles are the function of the surface charge, pH levels of aqueous solution and particle concentration; each variable is strongly interconnected. For example, the attractive van der Waals interaction between nanosized particles increases, as pH levels of aqueous solution approach the isoelectric point (IEP). This is due to the diminished electric double layer on the surface of each particle. In this study, both magnetites formed aggregates in aqueous solutions, even though the experiments were carried out under acidic conditions (~2.5 pH). IEP of the biogenic and commercial magnetites were determined to be 5.6 and 6.0, respectively. The biogenic magnetite tended to form approximately 4 times bigger aggregates in the reactor than the commercial one. This seems to be caused by the difference of surface charge on the surface of particles, because the surface charge and surface potential are related [15]. According to the electrophoretic mobility analysis, the surface zeta potential of the commercial magnetite was higher than that of the biogenic one; the higher the surface charge is, the higher the repulsive electric force between particles. In nanosized particles, the ratio of the surface area of the commercial and biogenic magnetites (surface area of commercial magnetite/surface area of biogenic magnetite) is 2.14; however, the ratio approaches 16 in aggregates under the assumption that all particles have spherical geometry and both magnetites have equal density. Therefore, this enhanced difference of surface area in aggregates would be responsible for the differences in the catalytic capacity of both magnetites.

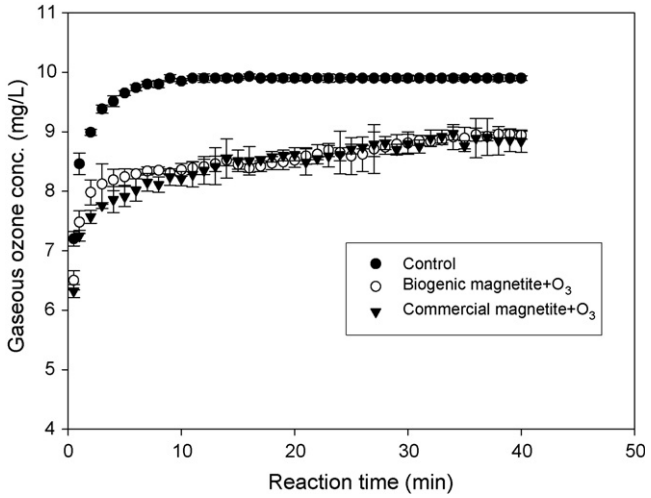

Fig. 6. Change of gaseous ozone concentration during reaction.

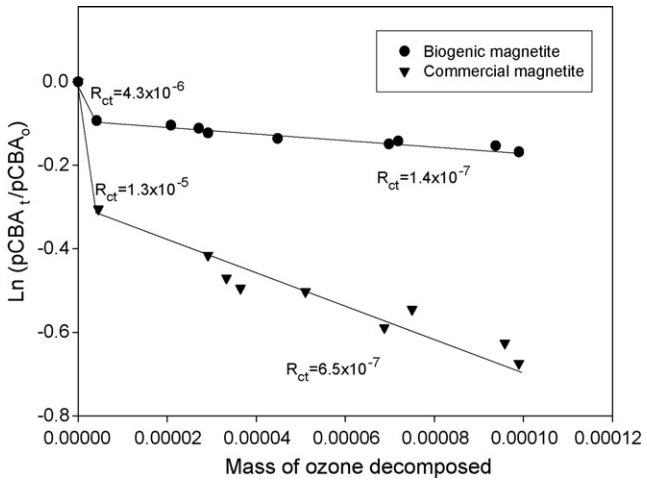

Fig. 7. Effect of catalysts on change of R_{ct} (conc. of gaseous ozone, *p*CBA, and iron oxide = 10, 2, and 56 mg/L, respectively).

The ozone concentration of off gas was monitored during reaction to test ozone demand of both magnetites, and the results are presented in Fig. 6. Gaseous ozone concentration in control experiment reached the steady state within 7 min of reaction. However, it took much longer time for the ozone concentration to reach the steady state in the presence of both magnetites. This result confirms that surface-catalyzed ozone decomposition reaction occurred. The commercial magnetite showed higher ozone demand than the biogenic one. Especially, the difference of gaseous ozone concentration between both magnetites is significant at the early of reaction. Commercial magnetite showed slightly higher removal rate than biogenic one at Phase I (Fig. 5). This *p*CBA oxidation result is consistent with the monitoring result of gaseous ozone concentration.

Elovitz and von Gunten [16] proposed the R_{ct} concept representing the ratio of the exposures of •OH radicals and ozone as follows:

$$R_{ct} = \frac{\int [^{\bullet}OH]\,dt}{\int [O_3]\,dt} \quad (1)$$

The R_{ct} implies the transformation efficiency of ozone into •OH radicals in the experimental system. The R_{ct} value can be determined by plotting *p*CBA degradation as a function of ozone exposure as Eq. (2).

$$\ln\left(\frac{[p\mathrm{CBA}]}{[p\mathrm{CBA}]_o}\right) = -k_{^{\bullet}OH/p\mathrm{CBA}} R_{ct} \int [O_3]\,dt \quad (2)$$

The R_{ct} values were determined with the biogenic and commercial magnetite. In the calculation of R_{ct} values, the amount of aqueous ozone consumed during reaction was estimated by submitting the off-gas ozone concentrations in control experiments without catalysts and off-gas ozone concentrations in experiments containing each catalyst. The results are shown in Fig. 7. In an attempt to estimate R_{ct} values from the slope, the each curve was simply divided into two subsections with linear regions. For both magnetites, the R_{ct} values during first period (1 min) were much greater than those during second period. For example, the R_{ct} value was estimated to be 4.3×10^{-6} during first period (1 min), and then it changed to 1.4×10^{-7} during second period for biogenic magnetite in the experimental conditions. This change of R_{ct} seems to be caused by initial rapid decrease of *p*CBA, as mentioned above. Commercial magnetite showed approximately 3.0 and 4.7 times greater R_{ct} values than biogenic magnetite during first period and second period, respectively.

4. Summary and conclusion

This study was carried out in order to characterize biogenic iron oxide and to evaluate its efficiency as a catalyst for heterogeneous catalytic ozonation. The experimental results with the biogenic iron oxide were compared with those of chemically same phase. The following conclusions are drawn on the basis of the experimental results and discussion:

- Nanosized biogenic iron oxide was successfully produced by dissimilatory iron-reducing bacterium, *Shewanella* sp. XRD and TEM analyses showed that biogenic iron oxide was magnetite phase (Fe_3O_4) in the range of 10.0 ± 4.0 nm in diameter.
- Catalytic ozonation was carried out at acidic pH levels (~2.5) in the presence of nanosized magnetite. The biogenic and commercial magnetites were found to enhance the degradation of *p*CBA via the production of •OH resulting from the catalytic decomposition of ozone.
- FT-IR and titration analyses confirmed that the biogenic magnetite contained functional groups on the surface originated from organic residual, and these functional groups played a role of basic group contents, which are considered the essential property of solid catalysts in the catalytic ozonation.
- However, the biogenic magnetite showed a lower catalytic efficiency than a commercial nanosized magnetite, although the commercial magnetite contained a lower basic group contents than the biogenic one. This result was caused by the formation of 4 times bigger aggregates of the biogenic magnetite than the commercial one in aqueous solutions. This implies that aggregate size in aqueous solutions significantly affect catalytic efficiency of the iron oxides.
- The R_{ct} values representing the ratio of hydroxyl radicals and ozone was estimated by dividing the non-linear curve into two subsections with linear regions. The R_{ct} values during first period (1 min) were much greater than those during second period, and this was caused by initial rapid decrease of *p*CBA.

Acknowledgement

This subject was supported by the Korea Science and Engineering Foundation (KOSEF) grant funded by the Korea government (MOST) (#M1050000012806J000012810).

References

[1] J.-S. Park, H. Choi, J. Choi, Water Res. 38 (2004) 2285.
[2] H. Jung, H. Choi, Appl. Catal. B-Environ. 66 (2000) 288.
[3] F.J. Beltran, F.J. Rivas, R. Montero-de-Espinosa, Ind. Eng. Chem. Res. 42 (2003) 3218.
[4] F.J. Beltran, F.J. Rivas, R. Montero-de-Espinosa, Water Res. 39 (2005) 3553.
[5] G.A. Waychunas, C.S. Kim, J.F. Banfiel, J. Nanopar. Res. 7 (2005) 409.
[6] F.R. Weiss, S.S. Kim, J.L. Kirschvink, R.E. Kopp, M. Sankaran, A. Kobayashi, A. Komeili, Earth Planet Sc. Lett. 224 (2004) 73.
[7] J.-H. Lee, Y. Roh, K.-W. Kim, H.-G. Hur, Geomicrobiol. J. 24 (2007) 31.
[8] B. Kasprzyk-Hordern, M. Ziolek, J. Nawrocik, Appl. Catal. B-Environ. 46 (2003) 639.
[9] M. Sanchez-Polo, U. von Gunten, J. Rivera-Utrilla, Water Res. 39 (2005) 3189.
[10] H. Jung, J. Kim, H. Choi, J. Environ. Eng.-ASCE 130 (2004) 432.
[11] W.-J. Huang, G.-C. Fang, C.-C. Wang, Colloid Surf. A 260 (2005) 45.
[12] H.-L. Lim, H. Choi, T.-M. Hwang, J.-W. Kang, Water Res. 36 (2004) 219.
[13] U. von Gunten, J. Hoigné, Environ. Sci. Techol. 28 (1994) 1234.
[14] E. Illes, E. Tombacz, J. Colloid Inter. Sci. 295 (2006) 115.
[15] W. Stumm, Chemistry of the Solid–Water Interface, Wiley, New York, 1992.
[16] M.S. Elovitz, U. von Gunten, Ozone-Sci. Eng. 21 (1999) 239.